Model Intestinal Microflora In Computer Simulation: A Simulation and Modelling Package for Host-Microflora Interactions

Michael H.F. Wilkinson, *Member, IEEE*

Abstract— **The ecology of the human intestinal microflora and its interaction with the host are poorly understood. Though more and more data are being acquired, in part using modern molecular methods, development of a quantitative theory has not kept pace with this increase in observing power. This is in part due to the complexity of the system, and to the lack of simulation environments in which to test what the ecological effect of a hypothetical mechanism of interaction would be, before resorting to laboratory experiments. The MIMICS project attempts to address this through the development of a cellular automaton for simulation of the intestinal microflora. In this paper the design and evaluation of this simulator are discussed.**

Keywords— **Computer simulation, microbial ecology, parallel computing, human intestines, intestinal microflora.**

I. Introduction

THE human intestines harbor a complex microbial ecosystem of an estimated 400 species, part bound to the intestinal wall or embedded in the mucus layer covering the wall, part inhabiting the lumen, especially of the large intestine. However, since the greater part (60-85 %) of the microscopically visible bacteria in faecal content cannot be cultured [1], the exact number of species, and even their nature and role in the ecosystem are not really known. The importance of the gut ecosystem stems from the fact that it is considered a first line of defense against invading pathogens. This effect, called colonization resistance (C.R.) [2], may be mediated through substrate competition, competition for wall binding sites, production of toxins by the resident microflora, etc. However, the precise mechanisms are poorly understood. The need to understand the intestinal microflora lies in the rapid and alarming increase in antibiotics resistance [3], [4], [5]. Increasingly, pathogenic bacteria are resistant to one or more antibiotics, causing problems in treatment of diseases such as tuberculosis [6], and closure of hospital wards contaminated by multiple resistant species such as methicilin resistant *Staphylococcus aureus* (MRSA) [5], [7]. Understanding the C.R. may offer alternatives to antibiotics [3], as is demonstrated in protection of poultry against pathogens by probiotics (live bacteria taken orally) [8].

Though simulation has been used in many fields of medicine such as surgery both for teaching and research purposes [9], [10], [11], and the earliest computer models of the intestinal microflora date from the early eighties [12], subsequently very little work has been done [13], [14], for a review see [15]. The Model Intestinal Microflora In Computer Simulation (MIMICS) project is the first attempt to model the human intestinal microflora by means of parallel high performance computers [15], [16]. The International Study Group for New Antimicrobial Strategies (ISGNAS, `www.isgnas.org`) [3] started the project for the above reasons. A pilot study [16] was performed to explore aerobe-anaerobe interactions in the gut from a theoretical point of view, and to test the feasibility of computer simulation in this area. However, no mathematical and implementation details of the simulator have yet been presented. Both issues will be dealt with in this paper.

This paper describes the development of the main tool: a large scale cellular automaton which can simulate both metabolic and transport processes in the human intestine. The program runs on the Cray J932 supercomputer of the Centre for High Performance Computing. In this simulator the model is broken up into five somewhat interrelated parts: (i) the bacterial metabolisms, (ii) the chemistry of the environment (food, oxygen supply, etc.), (iii) the geometry of the environment, (iv) the mechanics of transport, and (v) the interaction with the immune system. At this stage, the immune system will be left out of the model completely. A reason for eliminating the immune system from the model (apart from its complexity) is that the majority of bacteria in a healthy intestine do not seem to evoke an immune response, thus modeling them without an interaction may well be realistic. I will first describe the model of the bacterial metabolisms, followed by a discussion of the fluid dynamic modeling used. Finally, the results of simulations using this system, based on different competition strategies are presented and discussed. It will be shown that, though the model is still very crude, and much detail has been omitted, some salient features of the intestinal microflora can be reproduced by the model.

II. The Model

A. Bacterial Metabolisms: Substrate Competition

If we focus on the distinction between aerobic and anaerobic metabolisms bacteria can be classified into six more-or-less distinct types. Four grow in completely oxygen free conditions:

strict anaerobe: even very low concentrations of oxygen kill

Manuscript received December 5, 2001; revised April 17, 2002. This study was funded in part by the Institute for Microbiology and Biochemistry, Herborn-Dill, Germany, and in part by the International Study Group for New Antimicrobial Strategies.

The author is at the Institute for Mathematics and Computing Science, University of Groningen, P.O. Box 800, 9700 AV Groningen, The Netherlands (e-mail:michael@cs.rug.nl).

Publisher Item Identifier 10.1109/TBME.2002.803548.

them
moderate anaerobe: can survive low concentrations of oxygen
tolerant anaerobe: are unaffected by O_2.
facultative (an)aerobe: grow better with oxygen, but fairly well in absence of O_2
Two other types require oxygen for survival:
microaerophile: needs low concentrations of O_2 to survive; perishes at moderate concentrations.
strict aerobe: requires oxygen to grow; no toxic effects at normal levels
All these types of bacterial metabolism will be modeled with ordinary differential equations of the same general form, using the Monod formalism [17]. Though logistic growth has been used for modeling the intestinal microflora [13] and bacteriocin competition [18], for ease of mathematical analysis, it is well established that this is not a realistic model for bacterial growth [17]. The Monod model is one of the simplest realistic models, in which growth is modeled by Michaelis-Menten type kinetics [19], [17]. The equation we use to model growth is

$$\mu(S,O_2)=\left(\mu_{an}+\mu_{O_2}\frac{O_2}{K_R+O_2}\right)\frac{S}{K_S+S} - \kappa_{O_2}\frac{O_2}{K_T+O_2}-\mu_b, \tag{1}$$

in which μ is the growth rate per unit of bacterial biomass (s^{-1}), S the concentration of food substrate [mol/l], O_2 the oxygen concentration [mol/l], μ_{an} and μ_{O_2} are the maximum growth rates by anaerobic and aerobic metabolisms respectively. K_S is the half saturation rate food concentration [mol/l], K_R the half saturation respiration rate oxygen concentration [mol/l] and κ_{O_2} is the maximum oxygen kill rate, and K_T is the half saturation kill rate oxygen concentration, and, finally, μ_b is the maintenance energy term. The first term in (1) concerns oxygen dependent growth through food uptake. The second term models cell destruction by oxygen, the third maintenance costs.

Strict aerobes have a zero μ_{an}, and zero κ_{O_2}. Conversely, strict anaerobes have a positive μ_{an}, and negative μ_{O_2} and positive κ_{O_2}. Tolerant anaerobes have positive μ_{an}, and zero μ_{O_2} and κ_{O_2}. Facultatives have positive μ_{an}, and μ_{O_2} combined with zero κ_{O_2}, and, finally, microaerophiles have zero μ_{an}, and positive μ_{O_2} and κ_{O_2}. In an ecosystem with P species of bacteria, the differential equation for the concentration of the k^{th} species of bacteria X_k associated with growth rate μ_k is simply

$$\frac{dX_k}{dt}=\mu_k(S,O_2)X_k. \tag{2}$$

The equation must be combined with equations for food and oxygen use

$$\frac{dS}{dt}=\sum_{k=1}^{P}\left(-\left(V_{an,k}+V_{O_2,k}\frac{O_2}{K_{R,k}+O_2}\right)\frac{S}{K_{S,k}+S} + Y_{\kappa,k}\kappa_{O_2,k}\frac{O_2}{K_{T,k}+O_2}\right)X_k \tag{3}$$

with $V_{an,k}$ the maximum specific uptake rate of the anaerobic metabolism, $V_{O_2,k}$ the maximum specific uptake rate of the aerobic metabolism, and $Y_{\kappa,k}$ the yield of substrate per unit of bacteria killed by oxygen. The oxygen usage is

$$\frac{dO_2}{dt}=-\sum_{k=1}^{P}\left(\beta_{R,k}\frac{O_2}{K_{R,k}+O_2}\frac{S}{K_{S,k}+S} + \beta_{T,k}\frac{O_2}{K_{T,k}+O_2}\right)X_k \tag{4}$$

with $\beta_{R,k}$ and $\beta_{R,k}$ the maximum oxygen uptake rates due to aerobic metabolism and to the toxic effect on anaerobes or microaerophiles, respectively.

B. Bacterial Metabolisms: Bacteriocins

Bacteria are capable of producing toxins, called bacteriocins, which are harmless to the host, but highly toxic to competitors, either through inhibition or cell lysis [20], [21]. In modeling this type of interaction we follow Frank [18], except that we use the Monod model for growth, as in (1) instead of logistic growth. Suppose bacterium X_k produces toxin T at a constant rate $Y_{T,k}$. This means that its growth will be reduced proportionally:

$$\frac{dX_k}{dt}=(\mu_k(S,O_2)-Y_{T,k})X_k. \tag{5}$$

This cost may vary and be very small in practice, as is discussed by Dykes and Hastings [22]. If species X_l is sensitive to the toxin, its growth is reduced by a term proportional to the toxin concentration.

$$\frac{dX_l}{dt}=(\mu_l(S,O_2)-\kappa_{T,l}T)X_l. \tag{6}$$

We also assume that toxin is lost in this reaction, so the differential equation for T becomes

$$\frac{dT}{dt}=Y_{T,k}X_k-\beta_{T,l}TX_l, \tag{7}$$

in which $\beta_{T,l}$ is the rate constant for the loss of toxin due to its toxic effect on X_l. Note that we do not model a saturation kill rate, due to the relatively low concentrations of toxin. It is immediately clear that, if $\mu_k(S,O_2)=\mu_l(S,O_2)$, toxin production is only an advantage if $T>\frac{Y_{T,k}}{\kappa_{T,l}}$.

C. Spatial and temporal discretization

In reality the intestine has a highly complicated geometry, which must be simplified in this simulator. Whatever the complexity of the geometry, the topology is relatively simple: that of a single, unbranching tube. The model intestine is assumed to be an axisymmetric tube of length L, which is subdivided into M sections of length l in the axial direction and N equivolume concentric cylinders in the radial direction. Indices i and j are used to denote volume elements in radial and axial directions respectively.

The radius of the tube varies along the intestine. To achieve this we use an array of R_j for $j=0,1,\ldots,M$, and

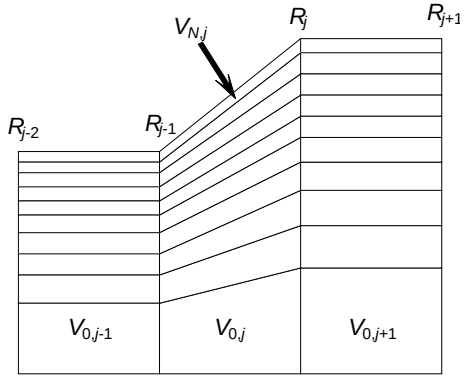

Fig. 1. A simple variable geometry: each axial section j has a trapezoidal shape determined by R_{j-1} and R_j.

in which each R_j pertains to the right edge of each axial section (see Fig. 1). Time dependence may be introduced by altering the contents of the array at every time step. The volume of element (i, j) becomes

$$V_{i,j} = \frac{\pi l(R_{j-1}^2 + R_{j-1}R_j + R_j^2)}{3N}, \tag{8}$$

The radial surface area of contact $A_{i,j,rad}$ between element (i, j) and $(i + 1, j)$ becomes

$$A_{i,j,rad} = \pi l(R_{j-1} + R_j)\sqrt{\frac{i}{N}}, \tag{9}$$

which depends on both i and j. The axial surface area of contact between element (i, j) and $(i, j + 1)$ is

$$A_{i,j,ax} = \frac{\pi R_j^2}{N}, \tag{10}$$

independent of i.

All simulations with the complete program were done with the following parameters: radial subdivisions $N = 10$, axial subdivisions $M = 100$, intestinal length $L = 6$ m with varying diameter; the first 4.98 m are the small intestine, with a radius of 1 cm; the next 18 cm are the "caecum" (radius 5 cm), followed by a "colon" of 84 cm long and 3 cm radius. This geometry can be seen in Figure 3. The number of radial subdivisions N influences the mean velocity in the volume elements along the wall, for the parabolic flow profile used (see section II-D.2). This in turn influences the wash-out of bacteria form the small intestine. For small N, the colonization of the small intestine decreased, whereas for $N > 10$ no qualitative changes were observed. The number of axial subdivisions M was chosen in a similar way. For small M it becomes harder to model the changes in radius along the intestinal length, whereas for large M no new features in the distribution of bacteria were observed.

The time scales of interest are in the order of days for the flora as a whole, and in the order of 20 min for the bacteria (fastest doubling time for *Escherichia coli*). The time step for the simulator was set at 5 min, after some experiments. Significantly longer time steps (20 min or more) could result in numerical instabilities, significantly shorter time steps (tested down to 10 s) did not appear to change the results in any significant way, except in CPU time needed to achieve them. It should be noted that time step for the the fourth-order Runge-Kutta ODE solver for the metabolism was adaptive. This was necessary because a time step of 5 min sometimes caused spurious oscillations due to negative concentrations appearing in the solution. When possible, a time step of 5 min was used, but if negative values were detected, the time step was shortened as necessary to avoid them. The performance of this adaptive strategy was validated in a simpler chemostat model, for which analytical solutions of the results are obtained readily. Furthermore, the result of simulations of batch fed cultures were compared to (much slower) stiff ODE solvers from the NAG library (Numerical Algorithms Group Ltd, Oxford, UK).

D. Transport Equations

The transport equations are modeled separately from the metabolism for two reasons. First of all, the geometry is such a coarse approximation of the real system that predicting the flow within this system accurately, using the Navier-Stokes equation, will not give us insight into the exact behavior of the real system. Secondly, it is easier to keep the design flexible, by separating reactions (the metabolism), from the transport component of the model. Therefore, the model contains only laminar flow for the bulk transport term, and diffusive mixing with a large diffusion rate constant for the mixing term.

D.1 Diffusion

Transport through diffusion applies to all volume elements. The process must be slow enough (or the time step must be short enough) to ensure that only diffusion between immediate neighbors need be considered. If this is the case, the diffusion of a substance s between two volume elements α and β is simply

$$\frac{ds(\alpha)}{dt} = \frac{\delta_s}{V_\alpha} A_{\alpha\beta} \frac{s(\beta) - s(\alpha)}{\Delta z}, \tag{11}$$

with $s(\alpha)$ and $s(\beta)$ the concentrations of s in volume elements α and β respectively, δ_s the diffusion coefficients of s, $A_{\alpha\beta}$ the surface area of contact between the volume elements, V_α the volume of element α, and Δz the distance between centers of gravity of volume elements. Because each volume element has 4 neighbors, we can obtain a difference equation

$$\begin{aligned}\Delta X_{k,i,j} =& w_{j-1}X_{k,i,j-1} + w_{j+1}X_{k,i,j+1} + \\ & w_{i-1}X_{k,i-1,j} + w_{i+1}X_{k,i+1,j} - w_0 X_{k,i,j},\end{aligned} \tag{12}$$

To obtain the weights w we divide each volume element into four subdivisions, each bordering on a single subdivision of one of its neighbors. We then compute the analytical solution of the differential equation (11) for each quarter volume element and its neighbor, and compute the mean

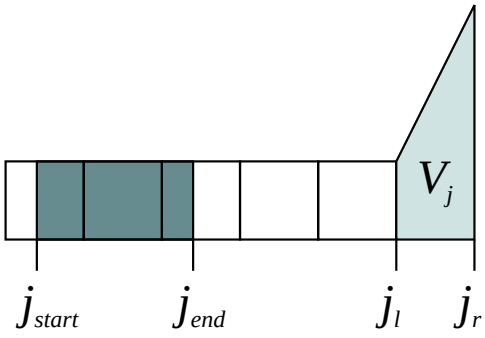

Fig. 2. Laminar flow: during time step Δt the shaded section between j_{start} and j_{end} moves to volume element V_j. Computing the concentration at $t+\Delta t$ in V_j reduces to computing j_{start} and j_{end} from the volume flow rate I, and computing the mean concentration in this area.

of these four solutions, yielding weights

$$w_{j-1,k} = V_{i,j-1}\frac{1-e^{-\frac{4(V_{i,j}+V_{i,j-1})A_{i,j-1,ax}}{lV_{i,j}V_{i,j-1}}\delta_k\Delta t}}{4(V_{i,j}+V_{i,j-1})}, \quad (13)$$

$$w_{i-1,k} = \frac{1-e^{-8\frac{A^2_{i-1,j,rad}}{V^2_{i,j}}\delta_k\Delta t}}{8}, \quad (14)$$

$$w_{j+1,k} = V_{i,j+1}\frac{1-e^{-\frac{4(V_{i,j}+V_{i,j+1})A_{i,j,ax}}{lV_{i,j}V_{i,j+1}}\delta_k\Delta t}}{4(V_{i,j}+V_{i,j+1})}, \quad (15)$$

$$w_{i+1,k} = \frac{1-e^{-8\frac{A^2_{i,j,rad}}{V^2_{i,j}}\delta_k\Delta t}}{8}, \quad (16)$$

and

$$w_{0,k} = w_{j-1,k} + w_{j+1,k} + w_{i-1,k} + w_{i+1,k}. \quad (17)$$

These weights can be computed at initialization, and stored in a sparse matrix representation. The diffusion subroutine only performs a single sparse matrix vector multiplication, which can be done in linear time, and parallelizes well.

D.2 Laminar flow

The next stage concerns laminar flow through the tube. In laminar flow the flow velocity as a function of radial position $v(r)$ is parabolic, which given our radial discretization becomes

$$v(i) = (v_{max} - v_{min})\left(1 - \frac{i-1}{N-1}\right) + v_{min}, \quad (18)$$

in terms of radial index i. We assume that the fluid flowing through the tube is incompressible, and each element's volume does not change in time. It is convenient to introduce the volume flow rate $I(i) = A_{i,j,ax}v_j(i)$, which has the same i-dependence as $v(i)$ in (18). Because the flow is laminar, we can compute the results of flow for each i independently, so we will leave i out of the further discussion. To compute the concentrations of substances in a given volume element V_j at $t+\Delta t$ from the distribution at t, we first find the leading and trailing edges of the volume which will occupy V_j at $t+\Delta t$. These are indicated by j_{end} and j_{start} respectively in Figure 2. The displaced volume in a time step Δt is $I\Delta t$, so that the j_{end} and j_{start} can be found by starting at the right-hand and left-hand boundaries j_r and j_l of V_j in Figure 2, and observing that

$$I\Delta t = \int_{j_{start}}^{j_l} A_{j,ax}\mathrm{d}j = \int_{j_{end}}^{j_r} A_{j,ax}\mathrm{d}j. \quad (19)$$

These integrals are of course approximated by sums, and can also be computed in advance. All that remains is to compute the mean concentration in the region between j_{start} and j_{end}.

E. Boundary conditions

Let us first consider the radial boundary at $i = N+1$. The boundary condition for O_2 is simplest: it can diffuse through the epithelium, and is always present in the epithelium, roughly at the level of oxygenated blood or tissue. Food behaves in a similar, but slightly more complex manner. Mucus containing nutrients is produced at an approximately constant rate. Uptake using Michaelis-Menten type kinetics was implemented, but was not used in these experiments. All other boundary conditions equate to hermetic sealing.

III. Simulations and Results

After initialization and input of experimental conditions (food and oxygen supply, bacterial metabolisms, etc.), the program will loop for a specified number of time steps through five subroutines which simulate (i) bacterial metabolism, (ii) laminar flow, (iii) diffusion, and (iv) store data and (v) report progress. Subroutines (i) through (iv) themselves loop through all elements of the i and j indices of the grid representing the intestine. After the loop ends, a final report is given and all files are closed.

In the simulation set-up and results, all concentrations are given in mol/l: food and all bacteria in moles of organic carbon, oxygen simply in moles of molecular oxygen (O_2). To convert to numbers of bacteria, it is assumed that the volume of a single bacterium was 10^{-15} l (i.e. a maximum of 10^{12}/g), and that they contain roughly 10 % w/w of organic C. This yields a conversion factor from mol/l to bacteria/g of about $1.2\cdot 10^{11}$. Using the MIMICS simulator, experiments were done to simulate colonization in a sterile intestine. One or two species of bacteria, selected from the available types (strict aerobe, facultative anaerobe and strict anaerobe, or toxin producer or susceptible), were introduced into a sterile intestine, in which the oxygen concentration of the lumen was in equilibrium with the walls (0.1 mmol/l). The input of food, oxygen, and bacteria was in block waves with a 40% duty cycle. Food concentration at maximum was 7 mol/l, oxygen concentration 0.1 mmol/l, and in most experiments the food inflow contained a maximum of $1.2\cdot 10^3$ bacteria/g of each species. Though this may be a bit high, runs with only 12 bacteria/g showed virtually identical results, so evidently

this parameter is relatively unimportant in the initial colonization phase. Varying the input substrate concentrations changes the steady-state concentrations of bacteria with anaerobic pathways (facultatives and strict anaerobes) linearly, whereas the steady-state concentration of strict aerobes is a linear function of the input oxygen concentrations (via wall and food).

A. Choice of parameter values

The metabolic parameters in (1) are listed in Table 1. The values given were derived in part from data obtained by Gerritse et al. [19]. Under aerobic conditions, the fastest growing bacteria can reach doubling times of about 20 min, which works out to a rate constant $\mu_{O_2} = 6 \cdot 10^{-4}$ s^{-1}. This value was used for strict aerobes. The maximum growth rate using an anaerobic metabolism $\mu_{an} = 1 \cdot 10^{-4}$ s^{-1} was derived from [19]. Though some species have a far lower μ_{an} (less than a division per day), it is unlikely that they could survive in an ecosystem with a dilution rate in the order of once per day. Strict anaerobes were therefore given a μ_{an} as above. For modeling facultatives, two different approaches were used: (i) the metabolism is a linear combination of the metabolisms for strict aerobes and strict anaerobes, with, with the sum of the weights assigned to each of the metabolic pathways equal to one, (ii) as (i), but with a sum of weights > 1. The rationale for the first model is that a bacterium has a limited enzyme budget to assign to each pathway, so the sum of weights should be one. The second model recognizes that in actual fact, the facultative anaerobe *E. coli* has a 20 min doubling time, combined with good anaerobic capability, which shows it grows faster than expected from the first model. In the second model, care must be taken not to create a "super bug": a bacterium which can simultaneously use both pathways at full capacity will always out-compete any other. The outcome of competition using both models is presented in the next section.

The Michaelis-Menten constants K_R and K_S were initially set at values found in [19]. However, these small values made the differential equations very stiff, resulting in long computation times. Because the influence of K_S on the outcome of the simulations lies mainly in the steady-state substrate concentration, and has little impact on the colonization itself [23], it can be set to much higher values with impunity, provided we are not interested in the steady-state substrate levels. For this reason, a value of $K_S = 0.02$ mol/l was used. Tests showed that the outcome of competition was virtually identical for values of K_S from 10^{-5} up to 0.02, as long as it is held equal for all competitors. The saturation constant K_R for oxygen cannot be treated in the same way, because the steady-state oxygen level determines the survival of strict anaerobes. Therefore, the value was set in the μmol/l range, following Wit et al. [24].

The basal metabolic parameter μ_b is more difficult to set, since less literature is available. If no toxic effects are present, the starvation time constant should not be smaller than about one day, or about 10^5 s. At the other extreme, bacteria might become dormant, thus avoiding starvation almost completely. Therefore, values of μ_b between 0 and $5 \cdot 10^{-6}$ s^{-1} were tested. Simulations run with either extreme setting of μ_b yielded only minor (3.5 %) differences in bacterial populations (lower with higher μ_b). No other changes were observed.

TABLE I
PARAMETERS DESCRIBING A BACTERIAL METABOLISM

Symbol	Meaning	Range	Units
μ_{O_2}	maximum aerobic growth rate	$-1.0 - 6.0 \cdot 10^{-4}$	/s
μ_{an}	maximum anaerobic growth rate	$0 - 1.0 \cdot 10^{-4}$	/s
μ_b	maintenance costs	$0 - 1 \cdot 10^{-5}$	/s
K_S	food uptake saturation constant	0.02	mol/l
K_R	respiratory oxygen uptake rate constant	$10^{-6} - 10^{-5}$	mol/l
K_T	toxic oxygen uptake rate constant	$10^{-6} - 10^{-5}$	mol/l
κ_{O_2}	maximum oxygen kill rate	$0 - 10^{-6}$	/s
κ_T	kill rate constant for toxin	$5 \cdot 10^{-6} - 5 \cdot 10^{-2}$	/mol /s
V_{O_2}	maximum aerobic food uptake rate	$-1 - 6 \cdot 10^{-4}$	/s
V_{an}	maximum anaerobic food uptake rate	$0 - 1.0 \cdot 10^{-4}$	/s
Y_κ	fraction of oxygen killed bacteria returned as food	$0.5 - 1$	
Y_T	Toxin production rate constant	$10^{-7} - 10^{-5}$	/s
β_μ	maximum respiratory oxygen uptake rate	$10^{-7} - 10^{-4}$	/s
β_κ	maximum oxygen uptake rate due to toxic effect	$0 - 1 \cdot 10^{-7}$	/s
β_T	toxin uptake rate constant due to toxic effect	$0 - 1 \cdot 10^{-8}$	/s

The substrate uptake rates were computed as the ratio of the maximum growth rate to the yield Y (unit of bacterial biomass per unit of substrate). The yield was set at 0.5, though values between 0.25 and 1 (perfect, lossless metabolism) were tested, and yielded similar results regarding the order of colonization. As expected, increasing the yield increases the steady-state bacterial densities linearly.

B. Aerobe-anaerobe interactions

In this set of simulations, the strict anaerobes, with $\mu_{an} = -\mu_{O_2} = 1 \cdot 10^{-4}/s$, $\kappa_{O_2} = 1 \cdot 10^{-6}/s$, and $K_T = K_R = 1 \cdot 10^{-6} mol/l$, competed with either facultative anaerobes modeled according to the methods outlined above, or with strict aerobes, with $\mu_{an} = 0$, $\mu_{O_2} = 6 \cdot 10^{-4}/s$, $\kappa_{O_2} = 0$, and $K_T = K_R = 1 \cdot 10^{-5} mol/l$. The results of some representative runs are shown in Figure 4.

In the first model for facultative behavior the weights given to the anaerobic and aerobic pathways w_{an} and w_{O_2} $(= 1 - w_{an})$ were varied, with μ_{an} ranging from 0.1 to 0.9. As the aerobic capacity decreased, the colonization slowed, due to the reduced speed of oxygen uptake. The top

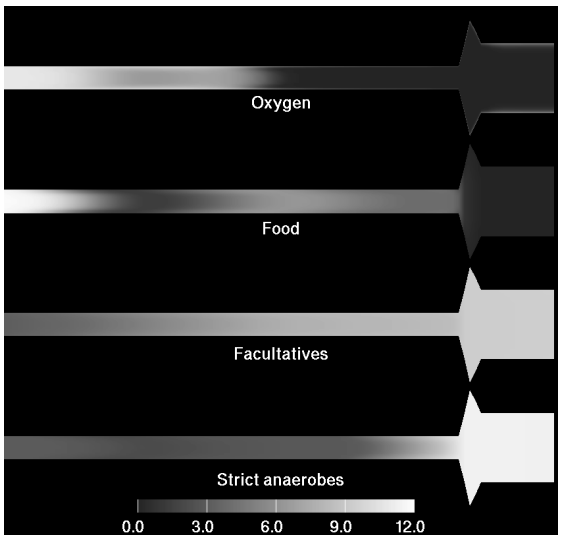

Fig. 3. The distribution of facultative anaerobes, strict anaerobes, food and oxygen 12 days after colonization, shown as 4 sections of the simulated intestine. The facultatives reach a concentration of some $5 \cdot 10^8$ in the large intestine, and are found in smaller numbers in the small intestine. The strict anaerobes grow out to $3 \cdot 10^{11}$ in the large intestine, and are present in very small numbers in the small intestine. Oxygen enters with the food, and along the walls, as can be seen in the top section.

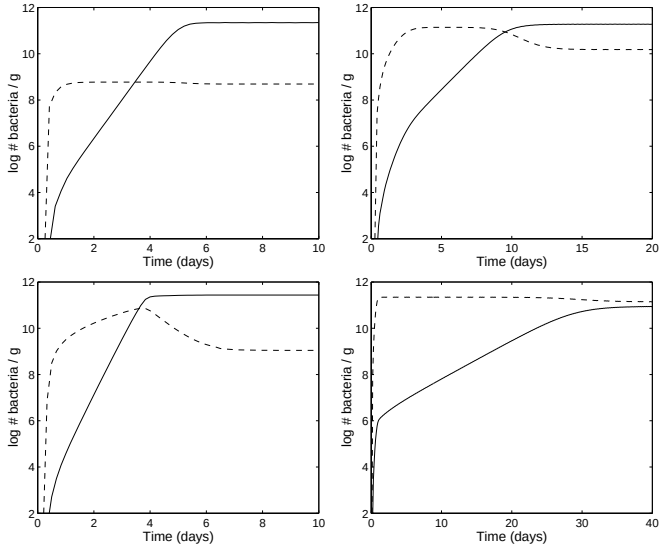

Fig. 4. Colonization process of two species of bacteria, one strict anaerobe (solid line) and one (facultative) aerobe (dashed). Four different situations are shown: (top left) strict aerobes; (top right) facultatives with $w_{an} = w_{O_2} = 0.5$; (bottom left) facultatives with $w_{an} = w_{O_2} = 0.75$; (bottom right) facultatives with $w_{an} = w_{O_2} = 0.9$. Initially, the aerobes colonize; later, as oxygen levels drop, the strict anaerobes out-compete the facultatives, except in the latter case. The sample point chosen here is in the center of the large intestine (indexes $j = 90$, $i = 1$).

righthand panel of Figure 4 shows the situation for $w_{an} = w_{O_2} = 0.5$. In the second model for facultative behavior, the weights for both pathways were kept equal, and ranged from 0.5 to 0.9. Only at the latter value did the facultatives become a "super-bug", out-competing the strict anaerobes. In that case, a two-species equilibrium did occur, but the facultatives outnumbered the strict anaerobes. This case, and the more realistic results for $w_{an} = w_{O_2} = 0.75$ are shown in Figure 4.

In all cases bacteria with aerobic pathways colonize first, followed by colonization by strict anaerobes. Once stabilized, the population did not change if the influx of bacteria from the "stomach" reduced to zero, thus they had colonized the lumen. The order of colonization in this experiment was observed by Schaedler et al. in mice [25], and similar patterns of colonization are observed in humans [26], [27], [28]. The distribution of bacteria and chemical species is shown schematically in Figure 3. It can clearly be seen how oxygen enters the lumen through the wall, and via the food. The facultative anaerobes dominate the small intestine, whereas the strict anaerobes dominate the large intestine. A further discussion of these results is given in [16].

C. Toxin mediated competition

In the case of toxin mediated competition, we modeled two tolerant anaerobic species, identical in their metabolic parameters, except in their ability to produce, and their resistance to a toxin T. Exact data on metabolic production and resistance costs are much rarer than maximum growth rates and saturation constants, so a wide range of parameter values was tested. A typical run is shown in 5. In this case, the producer X_k had a toxin yield $Y_T = 5 \cdot 10^{-7} s^{-1}$, which is a small percentage of its maintenance cost, and $\beta_T = \kappa_T = 0$. The sensitive species had $Y_T = 0$, and $\beta_T = 1 \cdot 10^{-9} s^{-1}$, which means little toxin is needed to destroy a single bacterium, and $\kappa_T = 5 \cdot 10^{-3} mol^{-1} s^{-1}$. Two situations were tested: (i) the toxin producer colonized first, after which the toxin-sensitive strain was ingested briefly , and (ii) the toxin sensitive strain colonized first, followed by ingestion of the toxin producer. As was found by Frank in a chemostat model [18], this type of interaction creates a first-come-first-serve ecosystem, in which the first arrival colonizes, and the second arrival fails to colonize. It comes as less of a surprise that in a toxin-filled intestine, the toxin-sensitive species fails to colonize, unless the toxin kill-rate is too small, so that $Y_T < \kappa_T T$. This is shown in Figure 7, where in the lefthand panel, the minimum effective toxin kill rate $\kappa_{T,min}$ is plotted as a function of steady-state producer density $X_{k,ss}$. Below this line, the cost of toxin production outweighs its effect on susceptibles. Increasing the yield does not help, because this raises toxin levels and costs equally.

However, it did turn out to be possible to replace toxin sensitive species which had colonized, by persistent addition of small numbers of producers to the food supply. In this case, the constant addition of producers overcomes the disadvantage of toxin production, and a sufficient number of producers builds up to produce sufficient toxin levels and replace the sensitives. This is shown in Figure 6. The reverse, replacing producers by susceptibles, was only possible for very high levels of ingested susceptibles. The minimum value $X_{l,min}$ which allows replacement was determined for a range of different steady-state population

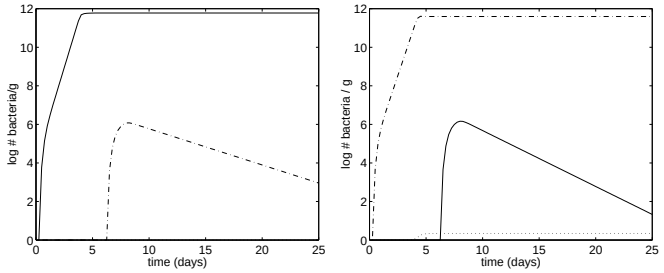

Fig. 5. Colonization patterns with toxin mediated competition: (left) 6 days after introduction of the toxin-sensitive species (solid line) to a sterile intestine, a toxin producer (dot-dash) is introduced; (right) the reverse experiment, in which the producer is introduced first, and toxin levels (dotted) become significant. In either case, the second species cannot out-compete the first.

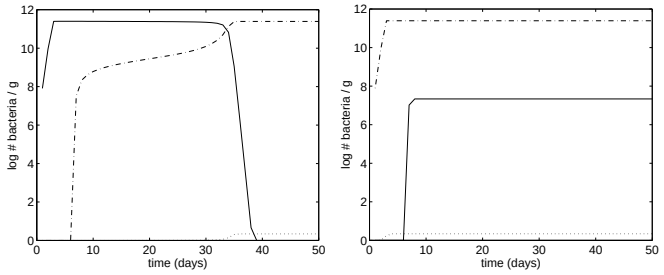

Fig. 6. Replacement of a colonized flora: (left) replacing toxin-sensitive bacteria (solid) by constant ingestion of producers (dot-dash) is possible; after day 35, significant levels of toxin (dotted) are present. By contrast (right) replacement of producers by constant ingestion of sensitives is harder to achieve.

densities $X_{k,ss}$ of toxin producers, for $\kappa_T = 5 \cdot 10^{-3}$, as is shown in the lefthand panel of 7.

Finally, the righthand panel of Figure 7 shows the necessary levels of producer ingested needed to replace susceptibles, as a function of Y_T. As Y_T decreases, $X_{k,min}$ decreases because a smaller growth disadvantage needs to be compensated. Varying the toxin uptake rate β_T mainly influences the time needed for invasion by producers, because a high value of β_T means more toxin is needed to destroy competitors.

The results are similar to what has been determined *in vitro* in well-mixed chemostats [29], [30], [31]. If very many toxin-sensitive bacteria are present, a few toxin producers cannot produce sufficient toxin to cause sufficient damage to the sensitive species, unless large numbers of producers invade [31]. In the case of ecosystems with distinct spatial structure, the situation is different, and sensitive and producing species may coexist, albeit in separate patches in the ecosystem [18], [29], [30]. In vivo data are less clear, though some studies do suggest colonization by toxin producers is possible in the intestine [32].

IV. Conclusions

Though care is needed when drawing conclusions from simulations only, and *in vitro* and *in vivo* data are needed to support them, they may be used to propose working hypotheses for new experiments at least. Furthermore, we may be able to infer which type of interaction is plausible,

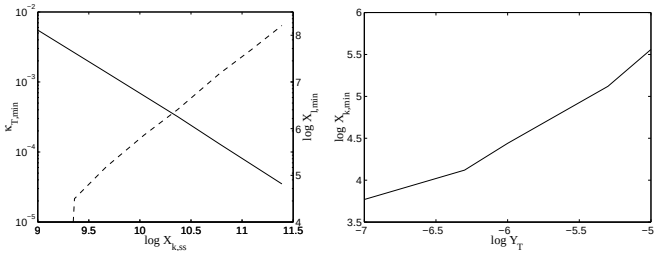

Fig. 7. Sensitivity to parameter values: (left) starting with a steady state population of producers $X_{k,ss}$, the minimum toxin kill rate $\kappa_{T,min}$ which prevents invasion (solid line), and the ($\log_{10}$) of the minimum density $X_{l,min}$ of ingested susceptible bacteria for successful invasion (dashed) are plotted as a function of $\log_{10} X_{k,ss}$ for $\kappa_{T,min} = 5 \cdot 10^{-3}$; (right) starting with a steady state population of susceptibles, the $\log_{10}$ of the minimum density $X_{k,min}$ of ingested producers for successful invasion as a function of ($\log_{10}$) toxin yield Y_T.

given specific observations. If we observe bi-stability of the kind exhibited by the toxin mediated competition model, it is at least unlikely that substrate mediated competition is important in that case, and this may direct us towards particular avenues of new research.

One hypothesis which is supported by our simulations, along with some *in vitro* and *in vivo* data [29], [30], [32], is that differences in colonization resistance (C.R.) between individuals may be due to the order in which they were initially colonized by toxin producers or susceptibles. According to the simulations, we might be able to boost the C.R. with appropriate probiotics. Whether this is the case in reality requires much more work, quite apart from the problem of finding suitable bacteria.

In the case of aerobe-anaerobe interactions, the order of colonization has little impact on the outcome of the simulation. Species with aerobe metabolisms are required to clear the way for anaerobes, by reducing the amount of oxygen available. After this, the anaerobes start to dominate the flora. This type of interaction and the mechanism have already been put forward by Schaedler et al. [25], and has been confirmed by numerous studies since then [26], [27], [28]. The numbers of anaerobes found in the large intestine ($3 \cdot 10^{11}$/g) is in line with what is observed, as is the ratio of anaerobes to aerobes ($10^3 : 1$) [33], except when unrealistic models for facultatives were used.

This report shows that it is possible to model the intestinal microflora and transport processes on the Cray J932 supercomputer, and its successor the SV1e in a comparatively simple program. The program parallelizes well, reaching speed-ups of about 8 on 10 CPUs, but only if the fourth-order Runge-Kutta solvers were used. The NAG library routines have side effects, which prevented them from running in parallel. Simulating 15 days cost between 10 minutes to 5 hours (depending on the interaction) of CPU time on the J932, which means between 2 and 40 minutes wall-clock time when 10 CPUs were used.

This work is just one of the first steps towards creating a simulation environment for modeling the intestinal microflora. Currently, work is in progress on the inclusion

of a proper mucosa [34], in which competition for binding sites can be simulated. The same paper demonstrates the possibility to monitor not only numbers of bacteria, but also their metabolic activity. It turned out that the most active part of the population is along the wall, which agrees with rRNA based measurements *insitu* by Poulsen et al [35]. Therefore, it is important to improve the realism of the wall of the simulator, including its fractal-like shape. True peristalsis and an immune system may be added at a later stage. In the future we hope to be able to provide researchers with an *in silico* experimental lab, which can assist in interpretation of *in vivo* and *in vitro* results, and in the design of new *in vivo* and *in vitro* experiments. Tight collaboration with these researchers is also necessary to provide further validation for the simulator. Finally, simulators such as these might be used for educational purposes, allowing students to visualize interactions between species.

Acknowledgments

The author would like to thank Drs R. de Bruin and J. Kraak of the Centre for High Performance Computing, University of Groningen, for many useful suggestions and discussions, and assistance with the visualization of the simulations, and Dr F. Schut, for many discussions on bacterial metabolism modeling.

References

[1] P. S. Langendijk, F. Schut, G. C. Raangs G.J. Jansen, G. Kamphuis, M. H. F. Wilkinson, and G. W. Welling, "Quantitative fluorescence in situ hybridization of Bifidobacterium spp. with genus-specific 16s rRNA-targeted probe and its application in fecal samples," *Applied and Environmental Microbiology*, vol. 61, pp. 3069–3075, 1995.

[2] D. van der Waaij, J. M. Berghuis-De Vries, and J. E. C. Lekkerkerk-Van der Wees, "Colonization resistance of the digestive tract in conventional and antibiotic treated mice," *Journal of Hygiene*, vol. 69, pp. 405–411, 1971.

[3] B. A. Araneo, J. J. Cebra, J. Beuth, R. Fuller, P. J. Heidt, T. Midvedt, C. E. Nord, P. Nieuwenhuis, W. L. Manson, G. Pulverer, V. C. Rusch, R. Tanaka, D. van der Waaij, R. I. Walker, and C. L. Wells, "Problems and priorities for controlling opportunistic pathogens with new antimicrobial strategies; an overview of current literature," *Zentralblad für Bakteriologie*, vol. 283, pp. 431–465, 1996.

[4] J. Davies, "Bacteria on the rampage.," *Nature*, vol. 383, pp. 219–220, 1996.

[5] M. A. Domin, "Highly virulent pathogens–a post antibiotic era?," *British Journal of Theatre Nursing*, vol. 8, no. 2, pp. 14–18, 1998.

[6] B. Petrini and S. Hoffner, "Drug-resistant and multidrug-resistant tubercle bacilli," *International Journal of Antimicrobial Agents*, vol. 13, pp. 93–97, 1999.

[7] D. Patel and I Madan, "Methicillin-resistant Staphylococcus aureus and multidrug resistant tuberculosis: Part 1," *Occupational Medicine*, vol. 50, pp. 392–394, 2000.

[8] D. J. Nisbet, D. E. Corrier, and J. R. DeLoach, "Effect of mixed cecal microflora maintained in continuous culture and of dietary lactose on Salmonella typhimurium colonization in broiler chicks," *Avian Disease*, vol. 37, pp. 528–535, 1993.

[9] L. M. Auer and D. P. Auer, "Virtual endoscopy for planning and simulation of minimally invasive neurosurgery," *Neurosurgery*, vol. 43, pp. 529–37, 1998.

[10] S.B. Issenberg, W. C. McGaghie, I. R. Hart, J. W. Mayer, J. M. Felner, E. R. Petrusa, R. A. Waugh, D. D. Brown, R. R. Safford, I. H. Gessner, D. L. Gordon, and G. A. Ewy, "Simulation technology for health care professional skills training and assessment," *JAMA*, vol. 282, pp. 861–866, 1999.

[11] J. Marescaux, J. M. Clement, V. Tassetti, C. Koehl, S. Cotin, Y. Russier, D. Mutter, H. Delingette, and N. Ayache, "Virtual reality applied to hepatic surgery simulation: the next revolution," *Annals of Surgery*, vol. 228, pp. 627–634, 1998.

[12] R. Freter, H. Brickner, J. Fekete, M. M. Vickerman, and K. V. Carey, "Survival and implantation of Escherichia coli in the intestinal tract," *Infection and Immunity*, vol. 39, pp. 686–703, 1983.

[13] M. E. Coleman, D. W. Dreesen, and R. G. Wiegert, "A simulation of microbial competition in the human colonic ecosystem," *Apllied and Environmental Microbiology*, vol. 62, pp. 3632–3639, 1996.

[14] D. E. Kirschner and M. J. Blaser, "The dynamics of Helicobacter pylori infection in the human stomach," *Journal of Theoretical Biology*, vol. 176, pp. 281–290, 1995.

[15] H. Boureau, L. Hartmann, T. Karjalainen, I. Rowland, and M. H. F. Wilkinson, "Models to study colonisation and colonisation resistance," *Microbial Ecology in Health and Disease*, vol. 12 suppl. 2, pp. 247–258, 2000.

[16] M. H. F. Wilkinson, "Nonlinear dynamics, chaos-theory, and the "sciences of complexity": their relevance to the study of the interaction between host and microflora.," in *Old Herborn University Seminar Monograph 10: New Antimicrobial Strategies*, P. J. Heidt, V. Rusch, and D. van der Waaij, Eds., Herborn-Dill, Germany, 1997, pp. 111–130, Herborn Litterae.

[17] A. L. Koch, "The Monod model and its alternatives," in *Mathematical Modeling in Microbial Ecology*, A. L. Koch, J. A. Robinson, and G. A. Milliken, Eds., pp. 62–93. Chapman & Hall, New York, 1998.

[18] S. A. Frank, "Spatial polymorphism of bacteriocines and other allelopathic traits," *Evol. Ecol.*, vol. 8, pp. 369–386, 1994.

[19] J. Gerritse, F. Schut, and J. C. Gottschal, "Modelling of mixed chemostat cultures of an anaerobic bacterium Comamonas testosteroni, and an anaerobic bacterium Veilonella alcalescencs: comparison with experimental data," *Applied and Environmental Microbiology*, vol. 58, pp. 1466–1476, 1992.

[20] M. A. Riley and D. M. Gordon, "The ecology and evolution of bacteriocins," *J. Ind. Microbiol.*, vol. 17, pp. 151–158, 1996.

[21] M. A. Riley, "Molecular mechanisms of bacteriocin evolution," *Ann. Rev. Genet.*, vol. 32, pp. 255–278, 1998.

[22] G. A. Dykes and J. W. Hastings, "Selection and fitness in bacteriocin-producing bacteria," *Proc. Royal Soc. London B*, vol. 264, pp. 683–687, 1997.

[23] J. Gottschal, "Growth kinetics and competition - some contemporary comments," *Antonie van Leeuwenhoek*, vol. 63, pp. 299–313, 1993.

[24] R. de Wit, F. P. van den Ende, and H. van Gemerden, "Mathematical simulation of the interactions among cyanobacteria, purple sulfur bacteria and chemotrophic sulfur bacteria in microbial mat communities," *FEMS Microbiology Ecology*, vol. 17, pp. 117–136, 1995.

[25] R. W. Schaedler, R. Dubos, and R. Costello, "Association of germfree mice with bacteria isolated from normal mice," *J. Exp. Med.*, vol. 122, pp. 77–82, 1963.

[26] P. L. Stark and A. Lee, "The microbial ecology of the large bowel of breast-fed and formula-fed infants during the first year of life," *J. Med. Microbiol.*, vol. 15, pp. 189–203, 1982.

[27] J. A. A. Hoogkamp-Korstanje, J. G. E. M. Lindner, J. H. Marcelis, H den Daas-Slagt, and N. M. de Vos, "Composition and ecology of the human intestinal flora," *Antonie van Leeuwenhoek*, vol. 45, pp. 335–340, 1979.

[28] I. Adlerberth, "Establishment of a normal intestinal microflora in the newborn infant," in *Probiotics, other Nutritional Factors and Intestinal Microflora*, L. A. Hanson and R. H. Yolken, Eds., Philadelphia, PA, 1999, pp. 63–78, Lippincott-Raven.

[29] L. Chao and B. R. Levin, "Structured habitats and the evolution of anticompetitor toxins in bacteria," *Proc. Natl. Acad. Sci. USA*, vol. 78, pp. 6324–6328, 1981.

[30] Y. Iwasa, M. Nakamaru, and S. A. Levin, "Allelopathy of bacteria in a lattice population: Competition between colicin-sensitive and colicin-producing strains," *Evol. Ecol.*, vol. 12, pp. 255–278, 1998.

[31] Y. Héchard, C. Jayat, F. Letellier, R. Julien, Y. Cenatiempo, and M. H. Ratinaud, "On-line visualization of the competitive behavior of antagonistic bacteria," *Applied and Environmental Microbiology*, vol. 58, pp. 3784–37866, 1992.

[32] A. D. Tadd and A. Hurst, "The effect of feeding colicinogenic Escherichia coli on the intestinal E. coli of early weaned pigs," *J. Appl. Bacteriol.*, vol. 24, pp. 222–228, 1961.

[33] B. Kleessen, E. Bezirtzoglou, and J. Mättö, "Culture-based

knowledge on biodiversity, development and stability of human gastrointestinal microflora," *Microbial Ecology in Health and Disease*, vol. 12 suppl. 2, pp. 54–63, 2000.

[34] D. J. Kamerman and M. H. F. Wilkinson, "In silico modelling of the human intestinal microflora," in *Proc. Int. Conf. Computational Science 2002*, Amsterdam, The Netherlands, April 21-24 2002, vol. 2329 of *Lecture Notes in Computer Science*, pp. 117–126.

[35] L. K. Poulsen, F. Lan, C. S. Kristensen, P. Hobolth, S. Molin, and K. A. Krogfelt, "Spatial distribution of Escherichia coli in the mouse large intestine inferred from rRNA in situ hybridization," *Infection and Immunity*, vol. 62, pp. 5191–5194, 1994.

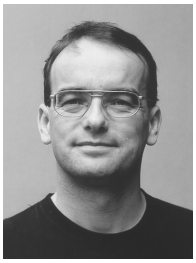

Michael Wilkinson obtained an MSc in astronomy from the Kapteyn Laboratory, University of Groningen (RuG) in 1993, after which he worked on image analysis of intestinal bacteria at the Department of Medical Microbiology, RuG. This work form the basis of his PhD at the Institute of Mathematics and Computing Science (IWI), RuG, in 1995. He was appointed as researcher at the Centre for High Performance Computing (also RuG) working on simulating the intestinal microbial ecosystem on parallel computers. During that time he edited the book "Digital Image Analysis of Microbes" (Wiley, 1998) together with Frits Schut. After this he worked as a researcher at the IWI on image analysis of diatoms, funded by European Commission MAST-contract MAS3-CT97-0122. He is currently assistant professor at the IWI.